

# Model for $J/\psi$ absorption in hadronic matter

Ziwei Lin and C. M. Ko

*Cyclotron Institute and Physics Department, Texas A&M University, College Station, Texas  
77843-3366*

## Abstract

The cross sections for  $J/\psi$  absorption by  $\pi$  and  $\rho$  mesons are studied in a meson-exchange model that includes not only pseudoscalar-pseudoscalar-vector-meson couplings but also three-vector-meson and four-point couplings. We find that they are much larger than in a previous study where only pseudoscalar-pseudoscalar-vector-meson couplings were considered. Including form factors at interaction vertices, the  $J/\psi$  absorption cross sections  $\sigma_{\pi\psi}$  and  $\sigma_{\rho\psi}$  are found to have values on the order of 7 mb and 3 mb, respectively. Their thermal averages in hadronic matter at temperature  $T = 150$  MeV are, respectively, about 1 mb and 2 mb.

PACS number(s): 25.75.-q, 14.40.Gx, 13.75.Lb

## I. INTRODUCTION

A dense partonic system, often called the quark-gluon plasma (QGP), is expected to be formed in heavy ion collisions at the Relativistic Heavy Ion Collider (RHIC), which will soon start to operate at the Brookhaven National Laboratory. Of all experimental observables that are sensitive to the presence of the QGP, charmonium is among the most promising ones. In particular, the dissociation of charmoniums in QGP due to color screening would lead to a reduction of their production in relativistic heavy ion collisions. The suppression of charmonium production in these collisions has thus been proposed as a possible signature for the formation of QGP [1]. Extensive experimental and theoretical efforts have been devoted to study this phenomenon [2–6]. However, available experimental data on  $J/\psi$  suppression in colliding systems ranging from  $pA$  to  $S+U$  are consistent with the scenario that charmoniums are absorbed by target and projectile nucleons with a cross section of about 7 mb [5]. Only in recent data from the Pb+Pb collision at  $P_{\text{lab}} = 158$  GeV/ $c$  in the NA50 experiment at CERN [4] is there a large additional  $J/\psi$  suppression in high  $E_T$  events, which requires the introduction of other absorption mechanisms. While there are suggestions that this anomalous suppression may be due to the formation of QGP [7,8], other more conventional mechanisms based on  $J/\psi$  absorption by comoving hadrons have also been proposed as a possible explanation [9,10]. Since the latter depends on the values of  $J/\psi$  absorption cross sections by hadrons, which are not known empirically, it is important to have better knowledge of the interactions between charmonium states and hadrons in order to understand the nature of the observed anomalous charmonium suppression.

Knowledge of  $J/\psi$  absorption cross sections by hadrons is also useful in estimating the contribution of  $J/\psi$  production from charm mesons in the hadronic matter formed in relativistic heavy ion collisions. Since the charm meson to  $J/\psi$  ratio in proton-proton collisions increases with energy, it has been shown that  $J/\psi$  production from hadronic matter may not be negligible in heavy ion collisions at the Large Hadronic Collider energies [11,12]. To use  $J/\psi$  suppression as a signature for the formation of QGP in these collisions thus requires the understanding of both  $J/\psi$  absorption and production in hadronic matter.

Various approaches have been used in evaluating the charmonium absorption cross sections by hadrons. In one approach, the quark-exchange model has been used. An earlier study based on this model by Martins, Blaschke, and Quack [13] has shown that the  $J/\psi$  absorption cross section  $\sigma_{\pi\psi}$  by pions has a peak value of about 7 mb at  $E_{\text{kin}} \equiv \sqrt{s} - m_{\pi} - m_{\psi} \simeq 0.8$  GeV, but a recent study by Wong, Swanson, and Barnes [14] gives a peak value of only  $\sigma_{\pi\psi} \sim 1$  mb at the same  $E_{\text{kin}}$  region. In the perturbative QCD approach, Kharzeev and Satz [15] have studied the dissociation of charmonium bound states by energetic gluons inside hadrons. They have predicted that the dissociation cross section increases monotonously with  $E_{\text{kin}}$  and has a value of only about 0.1 mb around  $E_{\text{kin}} \sim 0.8$  GeV. In the third approach, meson-exchange models based on hadronic effective Lagrangians have been used. Using pseudoscalar-pseudoscalar-vector-meson couplings (PPV couplings), Matinyan and Müller [16] have found  $\sigma_{\pi\psi} \simeq 0.3$  mb at  $E_{\text{kin}} = 0.8$  GeV. In a more recent study, Haglin [17] has included also the three-vector-meson couplings (VVV couplings) and four-point couplings (or contact terms), and obtained much larger values of  $J/\psi$  absorption cross sections. Large discrepancies in the magnitude of  $\sigma_{\pi\psi}$  (as well as  $\sigma_{\rho\psi}$ ) thus exist among the predictions from these three approaches, and further theoretical studies are needed. In the present study, we use a meson-exchange model as in Ref. [17] but treat differently the VVV and four-point couplings in the effective Lagrangian and also take into account the effect of form factors at interaction vertices.

Our paper is organized as follows. In Sec. II, we introduce the effective hadronic Lagrangian that we use to obtain the relevant interactions among  $J/\psi$  and hadrons. The cross sections for  $J/\psi$  absorption by  $\pi$  and  $\rho$  mesons are then evaluated. The amplitudes for the coherent sum of individual diagrams are checked to ensure that the hadronic current is conserved in the limit of zero vector meson masses. We then show in Sec. III the numerical results for the cross sections and their dependence on the form factors at interaction vertices. In Sec. IV, we compare our results with other models, and give more discussions on form factors and the effect due to the finite  $\rho$  meson width. A summary is also given in this section. In Appendix A, we discuss the determination of coupling constants based on the vector meson dominance model. More detailed comparisons with the approach used in Ref. [17] are given in Appendix B.

## II. $J/\psi$ ABSORPTION IN HADRONIC MATTER

### A. Effective Lagrangian

The free Lagrangian for pseudoscalar and vector mesons in the limit of SU(4) invariance can be written as

$$\mathcal{L}_0 = \text{Tr} \left( \partial_\mu P^\dagger \partial^\mu P \right) - \frac{1}{2} \text{Tr} \left( F_{\mu\nu}^\dagger F^{\mu\nu} \right) , \quad (1)$$

where  $F_{\mu\nu} = \partial_\mu V_\nu - \partial_\nu V_\mu$ , and  $P$  and  $V$  denote, respectively, the properly normalized  $4 \times 4$  pseudoscalar and vector meson matrices in SU(4) [18]:

$$P = \frac{1}{\sqrt{2}} \begin{pmatrix} \frac{\pi^0}{\sqrt{2}} + \frac{\eta}{\sqrt{6}} + \frac{\eta_c}{\sqrt{12}} & \pi^+ & K^+ & \bar{D}^0 \\ \pi^- & -\frac{\pi^0}{\sqrt{2}} + \frac{\eta}{\sqrt{6}} + \frac{\eta_c}{\sqrt{12}} & K^0 & D^- \\ K^- & \bar{K}^0 & -\sqrt{\frac{2}{3}}\eta + \frac{\eta_c}{\sqrt{12}} & D_s^- \\ D^0 & D^+ & D_s^+ & -\frac{3\eta_c}{\sqrt{12}} \end{pmatrix} ,$$

$$V = \frac{1}{\sqrt{2}} \begin{pmatrix} \frac{\rho^0}{\sqrt{2}} + \frac{\omega'}{\sqrt{6}} + \frac{J/\psi}{\sqrt{12}} & \rho^+ & K^{*+} & \bar{D}^{*0} \\ \rho^- & -\frac{\rho^0}{\sqrt{2}} + \frac{\omega'}{\sqrt{6}} + \frac{J/\psi}{\sqrt{12}} & K^{*0} & D^{*-} \\ K^{*-} & \bar{K}^{*0} & -\sqrt{\frac{2}{3}}\omega' + \frac{J/\psi}{\sqrt{12}} & D_s^{*-} \\ D^{*0} & D^{*+} & D_s^{*+} & -\frac{3J/\psi}{\sqrt{12}} \end{pmatrix} . \quad (2)$$

To obtain the couplings between pseudoscalar mesons and vector mesons, we introduce the minimal substitution

$$\partial_\mu P \rightarrow \mathcal{D}_\mu P = \partial_\mu P - \frac{ig}{2} [V_\mu P] , \quad (3)$$

$$F_{\mu\nu} \rightarrow \partial_\mu V_\nu - \partial_\nu V_\mu - \frac{ig}{2} [V_\mu, V_\nu] . \quad (4)$$

The effective Lagrangian is then given by

$$\begin{aligned} \mathcal{L} = \mathcal{L}_0 &+ \frac{ig}{2} \text{Tr} \left( \partial^\mu P [P^\dagger, V_\mu^\dagger] + \partial^\mu P^\dagger [P, V_\mu] \right) - \frac{g^2}{4} \text{Tr} \left( [P^\dagger, V_\mu^\dagger] [P, V^\mu] \right) \\ &+ \frac{ig}{2} \text{Tr} \left( \partial^\mu V^\nu [V_\mu^\dagger, V_\nu^\dagger] + \partial_\mu V_\nu^\dagger [V^\mu, V^\nu] \right) + \frac{g^2}{8} \text{Tr} \left( [V^\mu, V^\nu] [V_\mu^\dagger, V_\nu^\dagger] \right) . \end{aligned} \quad (5)$$

The hermiticity of  $P$  and  $V$  reduces this to

$$\begin{aligned} \mathcal{L} = \mathcal{L}_0 &+ ig \text{Tr} \left( \partial^\mu P [P, V_\mu] \right) - \frac{g^2}{4} \text{Tr} \left( [P, V_\mu]^2 \right) \\ &+ ig \text{Tr} \left( \partial^\mu V^\nu [V_\mu, V_\nu] \right) + \frac{g^2}{8} \text{Tr} \left( [V_\mu, V_\nu]^2 \right) . \end{aligned} \quad (6)$$

Since the SU(4) symmetry is explicitly broken by hadron masses, terms involving hadron masses are added to Eq.(6) using the experimentally determined values.

## B. Effective Lagrangians relevant for $J/\psi$ absorption

Expanding the Lagrangian in Eq.(6) explicitly in terms of the pseudoscalar meson and vector meson matrices shown in Eq.(2), we obtain the following interaction Lagrangians that are relevant for the study of  $J/\psi$  absorption by  $\pi$  and  $\rho$  mesons:

$$\mathcal{L}_{\pi DD^*} = ig_{\pi DD^*} D^{*\mu} \vec{\tau} \cdot \left( \bar{D} \partial_\mu \vec{\pi} - \partial_\mu \bar{D} \vec{\pi} \right) + \text{H.c.} , \quad (7)$$

$$\mathcal{L}_{\psi DD} = ig_{\psi DD} \psi^\mu \left( D \partial_\mu \bar{D} - \partial_\mu D \bar{D} \right) , \quad (8)$$

$$\begin{aligned} \mathcal{L}_{\psi D^* D^*} &= ig_{\psi D^* D^*} \left[ \psi^\mu \left( \partial_\mu D^{*\nu} \bar{D}_\nu^* - D^{*\nu} \partial_\mu \bar{D}_\nu^* \right) + \left( \partial_\mu \psi^\nu D_\nu^* - \psi^\nu \partial_\mu D_\nu^* \right) \bar{D}^{*\mu} \right. \\ &\quad \left. + D^{*\mu} \left( \psi^\nu \partial_\mu \bar{D}_\nu^* - \partial_\mu \psi^\nu \bar{D}_\nu^* \right) \right] , \end{aligned} \quad (9)$$

$$\mathcal{L}_{\pi \psi DD^*} = -g_{\pi \psi DD^*} \psi^\mu \left( D_\mu^* \vec{\tau} \bar{D} + D \vec{\tau} \bar{D}_\mu^* \right) \cdot \vec{\pi} , \quad (10)$$

$$\mathcal{L}_{\rho DD} = ig_{\rho DD} \left( D \vec{\tau} \partial_\mu \bar{D} - \partial_\mu D \vec{\tau} \bar{D} \right) \cdot \vec{\rho}^\mu ,$$

$$\mathcal{L}_{\rho \psi DD} = g_{\rho \psi DD} \psi^\mu D \vec{\tau} \bar{D} \cdot \vec{\rho}_\mu ,$$

$$\begin{aligned} \mathcal{L}_{\rho D^* D^*} &= ig_{\rho D^* D^*} \left[ \left( \partial_\mu D^{*\nu} \vec{\tau} \bar{D}_\nu^* - D^{*\nu} \vec{\tau} \partial_\mu \bar{D}_\nu^* \right) \cdot \vec{\rho}^\mu + \left( D^{*\nu} \vec{\tau} \cdot \partial_\mu \vec{\rho}_\nu - \partial_\mu D^{*\nu} \vec{\tau} \cdot \vec{\rho}_\nu \right) \bar{D}^{*\mu} \right. \\ &\quad \left. + D^{*\mu} \left( \vec{\tau} \cdot \vec{\rho}^\nu \partial_\mu \bar{D}_\nu^* - \vec{\tau} \cdot \partial_\mu \vec{\rho}^\nu \bar{D}_\nu^* \right) \right] , \end{aligned}$$

$$\mathcal{L}_{\rho \psi D^* D^*} = g_{\rho \psi D^* D^*} \left( \psi^\nu D_\nu^* \vec{\tau} \bar{D}_\mu^* + \psi^\nu D_\mu^* \vec{\tau} \bar{D}_\nu^* - 2\psi_\mu D^{*\nu} \vec{\tau} \bar{D}_\nu^* \right) \cdot \vec{\rho}^\mu . \quad (11)$$

In the above,  $\vec{\tau}$  are the Pauli matrices, and  $\vec{\pi}$  and  $\vec{\rho}$  denote the pion and rho meson isospin triplets, respectively, while  $D \equiv (D^0, D^+)$  and  $D^* \equiv (D^{*0}, D^{*+})$  denote the pseudoscalar and vector charm meson doublets, respectively. We note that exact SU(4) symmetry would give the following relations among the coupling constants in the Lagrangian:

$$\begin{aligned} g_{\pi DD^*} &= g_{\rho DD} = g_{\rho D^* D^*} = \frac{g}{4} , \quad g_{\psi DD} = g_{\psi D^* D^*} = \frac{g}{\sqrt{6}} , \\ g_{\pi \psi DD^*} &= g_{\rho \psi D^* D^*} = \frac{g^2}{4\sqrt{6}} , \quad g_{\rho \psi DD} = \frac{g^2}{2\sqrt{6}} . \end{aligned} \quad (12)$$

### C. $J/\psi$ absorption cross sections

The above effective Lagrangians allow us to study the following processes for  $J/\psi$  absorption by  $\pi$  and  $\rho$  mesons:

$$\pi\psi \rightarrow D^* \bar{D} , \quad \pi\psi \rightarrow D \bar{D}^* , \quad \rho\psi \rightarrow D \bar{D} , \quad \rho\psi \rightarrow D^* \bar{D}^* . \quad (13)$$

The corresponding diagrams for these processes, except the process  $\pi\psi \rightarrow D \bar{D}^*$ , which has the same cross section as the process  $\pi\psi \rightarrow D^* \bar{D}$ , are shown in Fig. 1.

The full amplitude for the first process  $\pi\psi \rightarrow D^* \bar{D}$ , without isospin factors and before summing and averaging over external spins, is given by

$$\mathcal{M}_1 \equiv \mathcal{M}_1^{\nu\lambda} \epsilon_{2\nu} \epsilon_{3\lambda} = \left( \sum_{i=a,b,c} \mathcal{M}_{1i}^{\nu\lambda} \right) \epsilon_{2\nu} \epsilon_{3\lambda} , \quad (14)$$

with

$$\begin{aligned} \mathcal{M}_{1a}^{\nu\lambda} &= -g_{\pi DD^*} g_{\psi DD} (-2p_1 + p_3)^\lambda \left( \frac{1}{t - m_D^2} \right) (p_1 - p_3 + p_4)^\nu , \\ \mathcal{M}_{1b}^{\nu\lambda} &= g_{\pi DD^*} g_{\psi D^* D^*} (-p_1 - p_4)^\alpha \left( \frac{1}{u - m_{D^*}^2} \right) \left[ g_{\alpha\beta} - \frac{(p_1 - p_4)_\alpha (p_1 - p_4)_\beta}{m_{D^*}^2} \right] \end{aligned}$$

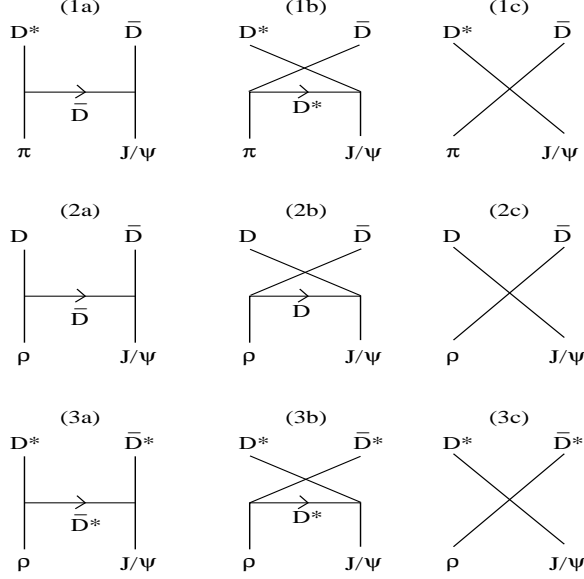


FIG. 1. Diagrams for  $J/\psi$  absorption processes: 1)  $\pi\psi \rightarrow D^*\bar{D}$ ; 2)  $\rho\psi \rightarrow D\bar{D}$ ; and 3)  $\rho\psi \rightarrow D^*\bar{D}^*$ . Diagrams for the process  $\pi\psi \rightarrow D\bar{D}^*$  are similar to (1a)-(1c) but with each particle replaced by its antiparticle.

$$\begin{aligned} & \times \left[ (-p_2 - p_3)^\beta g^{\nu\lambda} + (-p_1 + p_2 + p_4)^\lambda g^{\beta\nu} + (p_1 + p_3 - p_4)^\nu g^{\beta\lambda} \right], \\ \mathcal{M}_{1c}^{\nu\lambda} &= -g_{\pi\psi D D^*} g^{\nu\lambda}. \end{aligned} \quad (15)$$

Similarly, the full amplitude for the second process  $\rho\psi \rightarrow D\bar{D}$  is given by

$$\mathcal{M}_2 \equiv \mathcal{M}_2^{\mu\nu} \epsilon_{1\mu} \epsilon_{2\nu} = \left( \sum_{i=a,b,c} \mathcal{M}_{2i}^{\mu\nu} \right) \epsilon_{1\mu} \epsilon_{2\nu}, \quad (16)$$

with

$$\begin{aligned} \mathcal{M}_{2a}^{\mu\nu} &= -g_{\rho D D} g_{\psi D D} (p_1 - 2p_3)^\mu \left( \frac{1}{t - m_D^2} \right) (p_1 - p_3 + p_4)^\nu, \\ \mathcal{M}_{2b}^{\mu\nu} &= -g_{\rho D D} g_{\psi D D} (-p_1 + 2p_4)^\mu \left( \frac{1}{u - m_D^2} \right) (-p_1 - p_3 + p_4)^\nu, \\ \mathcal{M}_{2c}^{\mu\nu} &= g_{\rho\psi D D} g^{\mu\nu}. \end{aligned} \quad (17)$$

For the third process  $\rho\psi \rightarrow D^*\bar{D}^*$ , the full amplitude is given by

$$\mathcal{M}_3 \equiv \mathcal{M}_3^{\mu\nu\lambda\omega} \epsilon_{1\mu} \epsilon_{2\nu} \epsilon_{3\lambda} \epsilon_{4\omega} = \left( \sum_{i=a,b,c} \mathcal{M}_{3i}^{\mu\nu\lambda\omega} \right) \epsilon_{1\mu} \epsilon_{2\nu} \epsilon_{3\lambda} \epsilon_{4\omega}, \quad (18)$$

with

$$\mathcal{M}_{3a}^{\mu\nu\lambda\omega} = g_{\rho D^* D^*} g_{\psi D^* D^*} \left[ (-p_1 - p_3)^\alpha g^{\mu\lambda} + 2 p_1^\lambda g^{\alpha\mu} + 2 p_3^\mu g^{\alpha\lambda} \right] \left( \frac{1}{t - m_{D^*}^2} \right)$$

$$\begin{aligned}
& \times \left[ g_{\alpha\beta} - \frac{(p_1 - p_3)_\alpha (p_1 - p_3)_\beta}{m_{D^*}^2} \right] \left[ -2p_2^\omega g^{\beta\nu} + (p_2 + p_4)^\beta g^{\nu\omega} - 2p_4^\nu g^{\beta\omega} \right], \\
\mathcal{M}_{3b}^{\mu\nu\lambda\omega} &= g_{\rho D^* D^*} g_{\psi D^* D^*} \left[ -2p_1^\omega g^{\alpha\mu} + (p_1 + p_4)^\alpha g^{\mu\omega} - 2p_4^\mu g^{\alpha\omega} \right] \left( \frac{1}{u - m_{D^*}^2} \right) \\
& \times \left[ g_{\alpha\beta} - \frac{(p_1 - p_4)_\alpha (p_1 - p_4)_\beta}{m_{D^*}^2} \right] \left[ (-p_2 - p_3)^\beta g^{\nu\lambda} + 2p_2^\lambda g^{\beta\nu} + 2p_3^\nu g^{\beta\lambda} \right], \\
\mathcal{M}_{3c}^{\mu\nu\lambda\omega} &= g_{\rho\psi D^* D^*} \left( g^{\mu\lambda} g^{\nu\omega} + g^{\mu\omega} g^{\nu\lambda} - 2g^{\mu\nu} g^{\lambda\omega} \right). \tag{19}
\end{aligned}$$

In the above,  $p_j$  denotes the momentum of particle  $j$ . We choose the convention that particles 1 and 2 represent initial-state mesons while particles 3 and 4 represent final-state mesons on the left and right sides of the diagrams shown in Fig. 1, respectively. The indices  $\mu, \nu, \lambda$ , and  $\omega$  denote the polarization components of external particles while the indices  $\alpha$  and  $\beta$  denote those of the exchanged mesons.

After averaging (summing) over initial (final) spins and including isospin factors, the cross sections for the three processes are given by

$$\frac{d\sigma_1}{dt} = \frac{1}{96\pi s p_{i,\text{cm}}^2} \mathcal{M}_1^{\nu\lambda} \mathcal{M}_1^{*\nu'\lambda'} \left( g_{\nu\nu'} - \frac{p_{2\nu} p_{2\nu'}}{m_2^2} \right) \left( g_{\lambda\lambda'} - \frac{p_{3\lambda} p_{3\lambda'}}{m_3^2} \right), \tag{20}$$

$$\frac{d\sigma_2}{dt} = \frac{1}{288\pi s p_{i,\text{cm}}^2} \mathcal{M}_2^{\mu\nu} \mathcal{M}_2^{*\mu'\nu'} \left( g_{\mu\mu'} - \frac{p_{1\mu} p_{1\mu'}}{m_1^2} \right) \left( g_{\nu\nu'} - \frac{p_{2\nu} p_{2\nu'}}{m_2^2} \right), \tag{21}$$

$$\begin{aligned}
\frac{d\sigma_3}{dt} &= \frac{1}{288\pi s p_{i,\text{cm}}^2} \mathcal{M}_3^{\mu\nu\lambda\omega} \mathcal{M}_3^{*\mu'\nu'\lambda'\omega'} \left( g_{\mu\mu'} - \frac{p_{1\mu} p_{1\mu'}}{m_1^2} \right) \left( g_{\nu\nu'} - \frac{p_{2\nu} p_{2\nu'}}{m_2^2} \right) \\
& \times \left( g_{\lambda\lambda'} - \frac{p_{3\lambda} p_{3\lambda'}}{m_3^2} \right) \left( g_{\omega\omega'} - \frac{p_{4\omega} p_{4\omega'}}{m_4^2} \right), \tag{22}
\end{aligned}$$

with  $s = (p_1 + p_2)^2$ , and

$$p_{i,\text{cm}}^2 = \frac{[s - (m_1 + m_2)^2][s - (m_1 - m_2)^2]}{4s} \tag{23}$$

is the squared momentum of initial-state mesons in the center-of-momentum (c.m.) frame.

#### D. Current conservation

The effective Lagrangian in Eq. (6) is generated by minimal substitution, which is equivalent to treating vector mesons as gauge particles. To preserve the gauge invariance in the limit of zero vector meson masses thus leads to both VVV and four-point couplings in the Lagrangian. The gauge invariance also results in current conservation; i.e., in the limit of zero vector meson masses, degenerate pseudoscalar meson masses, and SU(4) invariant coupling constants, one has

$$\mathcal{M}_n^{\lambda_k \dots \lambda_l} p_{j\lambda_j} = 0, \tag{24}$$

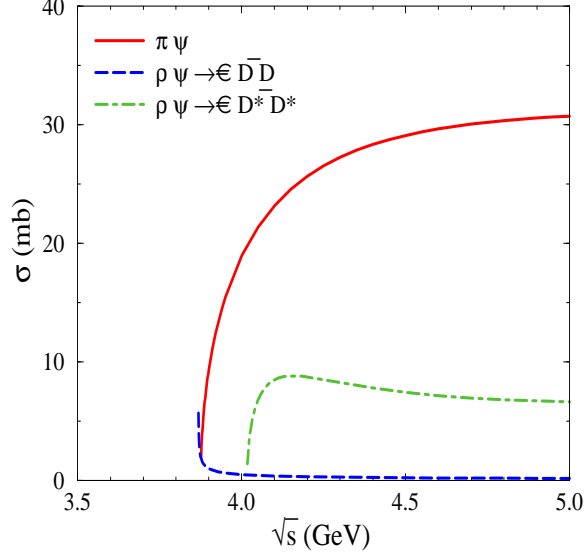


FIG. 2.  $J/\psi$  absorption cross section (without form factors) as a function of the c.m. energy of initial-state mesons. The solid curve represents the total contribution from both  $\pi\psi \rightarrow D^*\bar{D}$  and  $\pi\psi \rightarrow \bar{D}^*D$  processes.

where the index  $\lambda_j$  denotes the external vector meson  $j$  in process  $n$  shown in Fig. 1. This then requires, e.g.,  $\mathcal{M}_1^{\nu\lambda} p_{3\lambda} = 0$  and  $\mathcal{M}_3^{\mu\nu\lambda\omega} p_{2\nu} = 0$ . In Appendix B, we shall explicitly check that the amplitudes given in Eq. (15), as an example, satisfy the requirement of current conservation.

### III. NUMERICAL RESULTS

The coupling constant  $g_{\pi DD^*}$  can be determined from the  $D^*$  decay width [19], and this gives  $g_{\pi DD^*} = 4.4$ . Using the vector meson dominance (VMD) model, we can determine other three-point coupling constants. As shown in Appendix A, their values are

$$g_{\rho DD} = g_{\rho D^* D^*} = 2.52, \quad g_{\psi DD} = g_{\psi D^* D^*} = 7.64. \quad (25)$$

For the four-point coupling constants, there is no empirical information, and we thus use the SU(4) relations to determine their values in terms of the three-point coupling constants, i.e.,

$$g_{\pi\psi DD^*} = g_{\pi DD^*} g_{\psi DD}, \quad g_{\rho\psi DD} = 2 g_{\rho DD} g_{\psi DD}, \quad g_{\rho\psi D^* D^*} = g_{\rho D^* D^*} g_{\psi D^* D^*}. \quad (26)$$

To obtain analytical expressions for the cross sections so that they can be directly included into a computer code for numerical calculations, we have used the software package FORM [20] to contract all Lorentz indices in Eq. (22).

#### A. Without form factors

Figure 2 shows the cross section of  $J/\psi$  absorption by  $\pi$  and  $\rho$  mesons as a function of the c.m. energy  $\sqrt{s}$  of the two initial-state mesons. The cross section  $\sigma_{\pi\psi}$ , shown by the

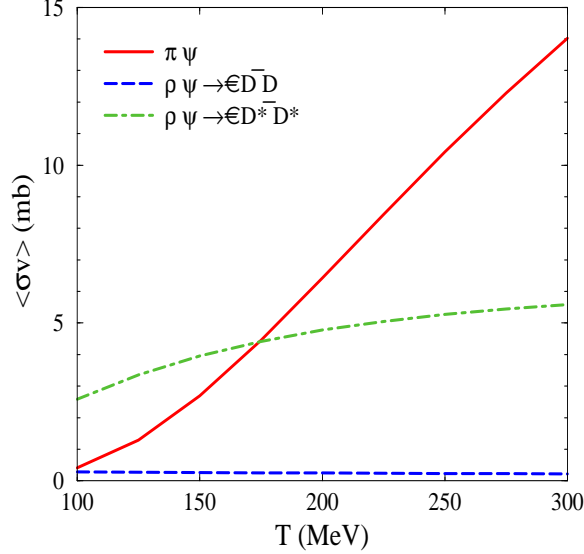


FIG. 3. Thermal average of  $J/\psi$  absorption cross section (without form factors) as a function of temperature  $T$ .

solid curve, includes contributions from both  $\pi\psi \rightarrow D\bar{D}^*$  and  $\pi\psi \rightarrow D^*\bar{D}$ , which have same cross sections. It is seen that the three  $J/\psi$  absorption cross sections have very different energy dependence near the threshold energy,  $\max(m_1 + m_2, m_3 + m_4)$ . While  $\sigma_{\pi\psi}$  increases monotonously with c.m. energy, the cross section for the process  $\rho\psi \rightarrow D\bar{D}$  decreases rapidly with c.m. energy, and that for the process  $\rho\psi \rightarrow D^*\bar{D}^*$  changes little with c.m. energy after an initial rapid increase near the threshold.

The thermal average of these cross sections in a hadronic matter at temperature  $T$  is given by

$$\langle\sigma v\rangle = \frac{\int_{z_0}^{\infty} dz [z^2 - (\alpha_1 + \alpha_2)^2] [z^2 - (\alpha_1 - \alpha_2)^2] K_1(z) \sigma(s = z^2 T^2)}{4\alpha_1^2 K_2(\alpha_1) \alpha_2^2 K_2(\alpha_2)}, \quad (27)$$

where  $\alpha_i = m_i/T$  ( $i = 1$  to  $4$ ),  $z_0 = \max(\alpha_1 + \alpha_2, \alpha_3 + \alpha_4)$ ,  $K_n$ 's are modified Bessel functions, and  $v$  is the relative velocity of initial-state particles in their collinear frame, i.e.,

$$v = \frac{\sqrt{(k_1 \cdot k_2)^2 - m_1^2 m_2^2}}{E_1 E_2}. \quad (28)$$

As shown in Fig. 3,  $\langle\sigma_{\pi\psi} v\rangle$  increases with increasing temperature, but  $\langle\sigma_{\rho\psi} v\rangle$  varies only moderately with temperature. The contribution of the process  $\rho\psi \rightarrow D\bar{D}$  to  $\langle\sigma_{\rho\psi} v\rangle$  is seen to decrease slightly with temperature. These features can be understood from the energy dependence of the cross sections shown in Fig. 2 and the difference in their kinematic thresholds (i.e.,  $m_3 + m_4 - m_1 - m_2$ ), which are about 0.64,  $-0.14$ , and 0.15 GeV for the processes  $\pi\psi \rightarrow D^*\bar{D}(D\bar{D}^*)$ ,  $\rho\psi \rightarrow D\bar{D}$ , and  $\rho\psi \rightarrow D^*\bar{D}^*$ , respectively. The process  $\pi\psi \rightarrow D^*\bar{D}(D\bar{D}^*)$  has the highest threshold, while the process  $\rho\psi \rightarrow D\bar{D}$  is exothermic and thus has no threshold. With a pion in the initial state, the process  $\pi\psi \rightarrow D^*\bar{D}(D\bar{D}^*)$  requires very energetic pions to overcome the high energy threshold and thus has a small thermal average  $\langle\sigma_{\pi\psi} v\rangle$  at low temperature. At higher temperature not only are there more



energetic pions that are able to overcome the kinematic threshold but also the cross section for the process  $\pi\psi \rightarrow D^*\bar{D}(D\bar{D}^*)$  increases with the c.m. energy as shown in Fig. 2;  $\langle\sigma_{\pi\psi}v\rangle$  thus increases strongly with temperature. For the process  $\rho\psi \rightarrow D\bar{D}$ , on the other hand, its contribution to the thermal average  $\langle\sigma_{\rho\psi}v\rangle$  decreases with temperature because with increasing temperature there are fewer rho mesons at low energy, which contribute the largest cross section. The contribution of the process  $\rho\psi \rightarrow D^*\bar{D}^*$  to  $\langle\sigma_{\rho\psi}v\rangle$  changes slowly with temperature as a result of both the small threshold and the fact that the cross section only weakly depends on the c.m. energy.

Compared with the results of Matinyan and Müller [16], we see that the inclusion of the VVV and four-point couplings increases  $\sigma_{\pi\psi}$  by an order of magnitude. For the process  $\rho\psi \rightarrow D\bar{D}$ , the decrease of its cross section after including four-point couplings is due to their destructive interference with the PPV coupling terms. The process  $\rho\psi \rightarrow D^*\bar{D}^*$  is entirely due to VVV and four-point couplings and is seen to have a much larger cross section than that for the process  $\rho\psi \rightarrow D\bar{D}$ . As a result, our effective Lagrangian including the VVV and four-point couplings also significantly increases  $\sigma_{\rho\psi}$ .

## B. With form factors

To take into account the composite nature of hadrons, form factors need to be introduced at interaction vertices. Unfortunately, there is no empirical information on form factors involving charmoniums and charm mesons. We thus take the form factors as the usual monopole form at the three-point  $t$  channel and  $u$  channel vertices, i.e.,

$$f_3 = \frac{\Lambda^2}{\Lambda^2 + \mathbf{q}^2}, \quad (29)$$

where  $\Lambda$  is a cutoff parameter, and  $\mathbf{q}^2$  is the squared three momentum transfer in the c.m. frame, given by  $(\mathbf{p}_1 - \mathbf{p}_3)_{\text{c.m.}}^2$  and  $(\mathbf{p}_1 - \mathbf{p}_4)_{\text{c.m.}}^2$  for  $t$  and  $u$  channel processes, respectively. We assume that the form factor at four-point vertices has the form

$$f_4 = \left( \frac{\Lambda_1^2}{\Lambda_1^2 + \bar{\mathbf{q}}^2} \right) \left( \frac{\Lambda_2^2}{\Lambda_2^2 + \bar{\mathbf{q}}^2} \right), \quad (30)$$

where  $\Lambda_1$  and  $\Lambda_2$  are the two different cutoff parameters at the three-point vertices present in the process with the same initial and final particles, and  $\bar{\mathbf{q}}^2$  is the average value of the squared three momentum transfers in  $t$  and  $u$  channels:

$$\bar{\mathbf{q}}^2 = \frac{[(\mathbf{p}_1 - \mathbf{p}_3)^2 + (\mathbf{p}_1 - \mathbf{p}_4)^2]_{\text{c.m.}}}{2} = p_{i,\text{c.m.}}^2 + p_{f,\text{c.m.}}^2. \quad (31)$$

For simplicity, we use the same value for all cutoff parameters, i.e.,

$$\Lambda_{\pi DD^*} = \Lambda_{\rho DD} = \Lambda_{\rho D^* D^*} = \Lambda_{\psi DD} = \Lambda_{\psi D^* D^*} \equiv \Lambda, \quad (32)$$

and choose  $\Lambda$  as either 1 or 2 GeV to study the uncertainties due to form factors.

Figure 4 shows the cross section as a function of the c.m. energy without and with form factors. It is seen that form factors strongly suppress the cross sections and thus cause large

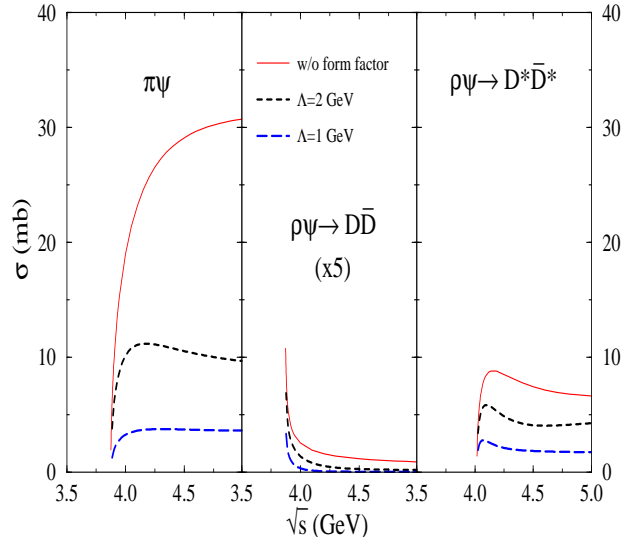


FIG. 4.  $J/\psi$  absorption cross section as a function of the c.m. energy of initial-state mesons with and without form factors.

uncertainties in their values. However, the  $J/\psi$  absorption cross sections remain appreciable after including form factors at interaction vertices. The values for  $\sigma_{\pi\psi}$  and  $\sigma_{\rho\psi}$  are roughly 7 mb and 3 mb, respectively, and are comparable to those used in phenomenological studies of  $J/\psi$  absorption by comoving hadrons in relativistic heavy ion collisions [9,10,21]. The thermal average of  $J/\psi$  absorption cross sections with and without form factors is shown in Fig. 5. At the temperature of 150 MeV, for example,  $\langle\sigma_{\pi\psi}v\rangle$  and  $\langle\sigma_{\rho\psi}v\rangle$  are about 1 mb and 2 mb, respectively.

#### IV. DISCUSSIONS AND SUMMARY

In our study, the effective Lagrangian shown in Eq. (6) is obtained from applying the minimal substitution of Eq. (3) and Eq. (4) to the free Lagrangian. The resulting PPV, VVV, and four-point (PPVV and VVVV) interaction Lagrangians in Eq. (6) are exactly the same as those in the chiral Lagrangian approach [22]<sup>1</sup>. They are, however, different from those used by Haglin [17]. The differences are shown in detail in Appendix B.

Values of the  $J/\psi$  absorption cross sections by hadrons obtained in our model are comparable to those from Martins, Blaschke, and Quack [13], Haglin [17], and Wong, Swanson, and Barnes [14], but are much larger than those from Kharzeev and Satz [15] and Matinyan and Müller [16]. As shown in Fig. 2 and Fig. 3, our results without form factors are much larger

---

<sup>1</sup>Before checking the identity of our effective Lagrangian to the corresponding ones in the chiral Lagrangian approach of Ref. [22], one should take notice of the different normalizations for the coupling constant  $g$  and the meson matrices as well as the following typos in that paper. The first part of Eq. (A2) in Ref. [22] should be  $U = \exp\left[i\frac{\sqrt{2}}{f_\pi}\phi\right]$ , Eq. (A3) should be  $D_\mu U = \partial_\mu U - igA_\mu^L U + igU A_\mu^R$ , and the first part of Eq. (A5) should be  $\mathcal{L}_{V\phi\phi}^{(3)} = -ig/2 \text{Tr}\partial_\mu\phi[V^\mu, \phi] + \dots$ .

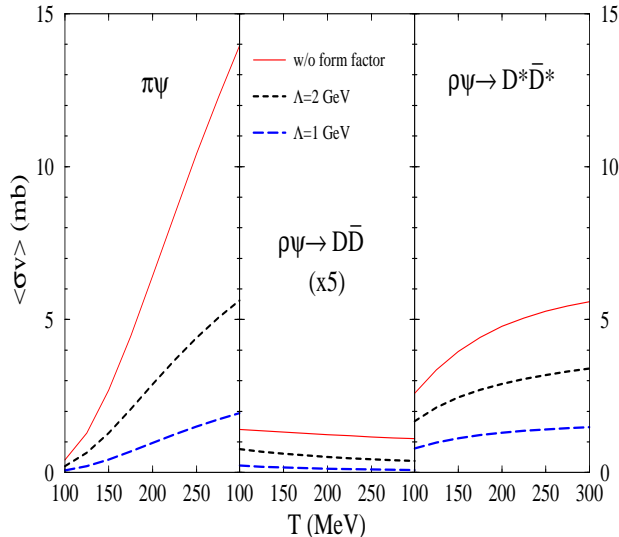


FIG. 5. Thermal-averaged cross section of  $J/\psi$  absorption as a function of temperature  $T$  with and without form factors.

than those from Matinyan and Müller [16] because the latter only included pseudoscalar-pseudoscalar-vector-meson couplings. As to the energy dependence of  $J/\psi$  absorption cross sections, our results shown in Fig. 2 for the case without form factors are similar to those from Matinyan and Müller [16] and Haglin [17], which are also based on effective hadronic Lagrangians. Including form factors weakens the energy dependence of the absorption cross sections as shown in Fig. 4. However, the decrease of the absorption cross sections with energy is still not as fast as in quark-exchange models [13,14]. This difference could be due to the fact that meson interactions in our effective hadronic Lagrangian approach involve derivative couplings, leading thus to a strong momentum dependence in the matrix elements, while the nonrelativistic potential used in the quark-exchange model does not have an explicit momentum dependence. Including the relativistic corrections to the quark-quark potential will be useful for further studying the energy dependence of the  $J/\psi$  absorption cross sections in the quark-exchange model.

Form factors involving charm mesons introduce significant uncertainties to our model based on hadronic effective Lagrangians, because there is little experimental information available. Four-point vertices appear in all processes in our study. If all vector mesons are massless, it is possible to determine the form factor at a four-point vertex once form factors at three-point vertices are chosen [23]. This is achieved through gauge invariance by requiring current conservation for the total amplitude that includes the form factors. Since the uncertainty of form factors involving charm mesons is already large for three-point vertices and the gauge invariance is only exact when all vector mesons are massless, we choose not to follow this more involved approach. Instead, we show the uncertainties due to form factors by using two different values for the cutoff parameters.

We have used the centroid value for the  $\rho$  meson mass in this study. Since the  $\rho$  meson width in vacuum is large (151 MeV), the threshold behavior of  $\rho\psi$  processes may change significantly with the  $\rho$  meson mass. E.g., a rho meson with mass below 630 MeV changes the process  $\rho\psi \rightarrow D\bar{D}$  from exothermic to endothermic, and the energy dependence of the

cross section near the threshold may thus change from fast decreasing (the dashed curve) shown in Fig. 2 to fast rising (similar to the dot-dashed curve). On the other hand, a rho meson with mass above 920 MeV changes the process  $\rho\psi \rightarrow D^*\bar{D}^*$  from endothermic to exothermic. We thus expect that the final value of the  $J/\psi$  absorption cross section by rho mesons will be different once the  $\rho$  meson width is considered. However, the  $\rho$  meson spectral function is further modified in the hadronic matter produced in heavy ion collisions [24,25], so the effects of the rho meson width on  $J/\psi$  absorption in hadronic matter are more involved. We therefore leave the effect of the  $\rho$  meson width on charmonium absorption to a future study.

Finally, vector mesons are treated as gauge particles in our approach. Since the SU(4) symmetry is not exact, it is not clear to what extent they can be treated as gauge particles. An alternative approach [26] based on both chiral symmetry and heavy quark effective theory may be useful in understanding the meson-exchange model we have used here.

In summary, we have studied the  $J/\psi$  absorption cross sections by  $\pi$  and  $\rho$  mesons in a meson-exchange model that includes pseudoscalar-pseudoscalar-vector-meson couplings, three-vector-meson couplings, and four-point couplings. We find that these cross sections have much larger values than in a previous study, where only pseudoscalar-pseudoscalar-vector-meson couplings were considered. Including form factors at the interaction vertices, the values for  $\sigma_{\pi\psi}$  and  $\sigma_{\rho\psi}$  are on the order of 7 mb and 3 mb, respectively, and their thermal averages at the temperature of 150 MeV are roughly 1 mb and 2 mb, respectively. These values are comparable to those used in the phenomenological studies of  $J/\psi$  absorption in relativistic heavy ion collisions. Our results thus suggest that the absorption of  $J/\psi$  by comoving hadrons may play an important role in the observed suppression.

## ACKNOWLEDGMENTS

We thank K. Haglin and C. Y. Wong for helpful communications. This work was supported in part by the National Science Foundation under Grant No. PHY-9870038, the Welch Foundation under Grant No. A-1358, and the Texas Advanced Research Program under Grants Nos. FY97-010366-0068 and FY99-010366-0081.

## APPENDIX A

In this appendix, we determine the values of the coupling constants within the framework of the VMD model. In the VMD model, the virtual photon in the process  $e^- D^+ \rightarrow e^- D^+$  is coupled to vector mesons  $\rho, \omega$ , and  $J/\psi$ , which are then coupled to the charm meson. At zero momentum transfer, the following relation holds:

$$\sum_{V=\rho,\omega,\psi} \frac{\gamma_V g_{VD^+D^-}}{m_V^2} = e. \quad (\text{A1})$$

In the above,  $\gamma_V$  is the photon-vector-meson mixing amplitude and can be determined from the vector meson partial decay width to  $e^+e^-$ , i.e.,

$$\Gamma_{Vee} = \frac{\alpha \gamma_V^2}{3m_V^3}, \quad (\text{A2})$$

with the fine structure constant  $\alpha = e^2/4\pi$ . The relative signs of  $\gamma_V$ 's can be determined from the hadronic electromagnetic current expressed in terms of quark currents [27]. Since the virtual photon sees the charge of charm quark in the charm meson through the  $\psi DD$  coupling, we have the following relations:

$$\frac{\gamma_\psi g_{\psi D^+D^-}}{m_\psi^2} = \frac{2}{3}e, \quad \frac{\gamma_\rho g_{\rho D^+D^-}}{m_\rho^2} + \frac{\gamma_\omega g_{\omega D^+D^-}}{m_\omega^2} = \frac{1}{3}e. \quad (\text{A3})$$

Similarly, one has, from the process  $e^- D^0 \rightarrow e^- D^0$ ,

$$\frac{\gamma_\psi g_{\psi D^0\bar{D}^0}}{m_\psi^2} = \frac{2}{3}e, \quad \frac{\gamma_\rho g_{\rho D^0\bar{D}^0}}{m_\rho^2} + \frac{\gamma_\omega g_{\omega D^0\bar{D}^0}}{m_\omega^2} = -\frac{2}{3}e. \quad (\text{A4})$$

Using  $g_{\rho D^+D^-} = -g_{\rho D^0\bar{D}^0} = g_{\rho DD}$ ,  $g_{\omega D^+D^-} = g_{\omega D^0\bar{D}^0} = g_{\omega DD}$ , and  $g_{\psi D^+D^-} = g_{\psi D^0\bar{D}^0} = g_{\psi DD}$  from isospin symmetry, we then have

$$\frac{\gamma_\psi g_{\psi DD}}{m_\psi^2} = \frac{2}{3}e, \quad \frac{\gamma_\rho g_{\rho DD}}{m_\rho^2} + \frac{\gamma_\omega g_{\omega DD}}{m_\omega^2} = \frac{1}{3}e, \quad -\frac{\gamma_\rho g_{\rho DD}}{m_\rho^2} + \frac{\gamma_\omega g_{\omega DD}}{m_\omega^2} = -\frac{2}{3}e. \quad (\text{A5})$$

From the above equations, we obtain the following coupling constants:

$$g_{\rho DD} = 2.52, \quad g_{\omega DD} = -2.84, \quad g_{\psi DD} = 7.64. \quad (\text{A6})$$

We note that in Ref. [16] the same VMD relations for  $g_{\rho DD}$  and  $g_{\psi DD}$  as our Eq. (A5) are used but slightly different values, i.e.,  $g_{\rho DD} = 2.8$  and  $g_{\psi DD} = 7.7$ , are obtained.

Equations similar to Eq. (A5) can be written for kaons and pions in order to obtain  $g_{VKK}$  and  $g_{V\pi\pi}$ . The resulting coupling constants, multiplied by the corresponding prefactors in the following SU(4) relations, are given in the parentheses for comparison:

$$g_{\rho\pi\pi}(5.04) = 2g_{\rho KK}(5.04) = 2g_{\rho DD}(5.04) = \frac{\sqrt{6}}{2}g_{\psi DD}(9.36). \quad (\text{A7})$$

We note that  $|g_{\rho\pi\pi}|$  is 6.06 if it is determined from the  $\rho$  meson decay width to two pions. It is seen that the predicted values differ only slightly from the above SU(4) relation except the coupling constant  $g_{\psi DD}$ . This may indicate a sizable uncertainty in the  $\psi DD$  coupling.

## APPENDIX B

In this appendix, we discuss in detail the differences between our approach and that of Ref. [17]. In particular, we compare the general effective Lagrangian for interacting pseudoscalar and vector mesons and the specific interaction Lagrangians for  $J/\psi$  scattering by pion and rho meson in the two approaches. We also examine the condition of current conservation for the amplitudes derived from the two approaches.

### A. General effective Lagrangian

In both approaches, one starts from the same free Lagrangian of Eq. (1). But our matrices for  $P$  and  $V$  differ from those of Ref. [17] by a factor of  $1/\sqrt{2}$  as given recently in Ref. [28]. For the minimal substitutions given in Eq. (3) and Eq. (4) for obtaining the interaction Lagrangians, the first one is the same in the two approaches but the second one is different. Instead of the factor  $g/2$  in the last term of Eq. (4), Ref. [17] uses  $g$ . As a result, the effective Lagrangian given by Eq. (2) in Ref. [17] has the following form:

$$\begin{aligned}
 l_{\text{int}} &= ig\text{Tr}(PV^\mu\partial_\mu P - \partial^\mu PV_\mu P) + \frac{1}{2}g^2\text{Tr}(PV^\mu V_\mu P - PV^\mu PV_\mu) \\
 &\quad + ig\text{Tr}(\partial^\mu V^\nu [V_\mu, V_\nu] + [V^\mu, V^\nu] \partial_\mu V_\nu) + g^2\text{Tr}(V^\mu V^\nu [V_\mu, V_\nu]) , \\
 &= ig\text{Tr}(\partial^\mu P [P, V_\mu]) - \frac{g^2}{4}\text{Tr}([P, V_\mu]^2) + 2ig\text{Tr}(\partial^\mu V^\nu [V_\mu, V_\nu]) + \frac{g^2}{2}\text{Tr}([V_\mu, V_\nu]^2) . \quad (\text{B1})
 \end{aligned}$$

This Lagrangian differs from ours in the three- (VVV) and four- (VVVV) vector meson couplings. Compared with our Eq. (6), we find that our VVV and VVVV terms are a factor of 2 and 4 smaller than corresponding ones in Ref. [17], respectively.

We note that the above differences in the effective Lagrangians used in the two approaches cannot be due to a redefinition of fields. To see this, we rescale the coupling  $g$  and the fields  $P$  and  $V$  by  $c_g, c_P$ , and  $c_V$ , *separately*, then the relative ratios of the PVV, PPVV, VVV, and VVVV terms are given by

$$c_g c_P^2 c_V, \quad c_g^2 c_P^2 c_V^2, \quad 2c_g c_V^3, \quad \text{and} \quad 4c_g^2 c_V^4. \quad (\text{B2})$$

It is obvious that these ratios cannot be changed to 1 simultaneously, as one needs  $c_g c_V = 1$  from the ratio of the first two terms but  $2c_g c_V = 1$  from the ratio of the last two terms.

### B. Lagrangians for the $J/\psi$ interaction with pions and rho mesons

After expanding the general effective Lagrangian, we have Eq. (7) for the  $\pi DD^*$  interaction, which should be compared with the following one in Ref. [17]:

$$l_{\pi DD^*} = \frac{i}{2}g'_{\pi DD^*} \left( \bar{D}\tau_i D^{*\mu} \partial_\mu \pi_i - \partial_\mu \bar{D}\tau_i D_\mu^* \pi_i - \text{H.c.} \right) , \quad (\text{B3})$$

where we have use  $g'$  to label the coupling constant in Ref. [17]. It is seen that our coupling constant  $g_{\pi DD^*}$  is a factor of 2 smaller. Apart from the possible difference due to the definition of  $D$  field, we have the same  $\mathcal{L}_{\pi DD^*}$  as Ref. [17].

Compared to our  $\psi DD$  interaction Lagrangian in Eq. (8), Ref. [17] has

$$l_{\psi DD} = ig'_{\psi DD} \psi^\mu \left[ \bar{D} \partial_\mu D - (\partial_\mu \bar{D}) D \right]. \quad (\text{B4})$$

Apart from a possible sign difference in the definition of  $g_{\psi DD}$ , both have the same  $\mathcal{L}_{\psi DD}$ .

Instead of our  $\psi D^* D^*$  interaction Lagrangian in Eq. (9), Ref. [17] has

$$l_{\psi D^* D^*} = -ig'_{\psi D^* D^*} \psi^\mu \left[ \bar{D}^{*\nu} (\partial_\mu D_\nu^*) - (\partial_\mu \bar{D}^{*\nu}) D_\nu^* - (\partial_\nu D_\mu^*) \bar{D}^{*\nu} + (\partial_\nu \bar{D}_\mu^*) D^{*\nu} \right]. \quad (\text{B5})$$

Besides a possible sign difference in the definition of  $g_{\psi D^* D^*}$ , we have two more terms in  $\mathcal{L}_{\psi D^* D^*}$ , which involve the derivative of the  $J/\psi$  field, than in Ref. [17]. We note that the cyclic form of our  $\mathcal{L}_{\psi D^* D^*}$  yields the following factor for the three-vector meson vertex in a Feynman diagram:

$$(p_1 - p_2)_\gamma g_{\mu\nu} + (p_2 - p_3)_\mu g_{\nu\gamma} + (p_3 - p_1)_\nu g_{\gamma\mu}, \quad (\text{B6})$$

which looks exactly like the structure of the three-gluon vertex in QCD. A similar difference appears between our approach and that of Ref. [17] for the  $\rho D^* D^*$  interaction Lagrangian. We note that there may be typos in Ref. [17] for  $l_{\psi D^* D^*}$  and  $l_{\rho D^* D^*}$ , as  $\bar{D}^* D^*$  and  $D^* \bar{D}^*$  cannot be both scalar.

For the  $\pi\psi DD^*$  interaction Lagrangian, ours is given by Eq.(10) while that in Ref. [17] is

$$l_{\psi\pi DD^*} = -g'_{\psi DD} g'_{\pi DD^*} \psi^\mu D_\mu^* \tau_i \bar{D} \pi_i, \quad (\text{B7})$$

which is non-Hermitian and thus likely contains a typo.

### C. Current conservation for $\pi\psi \rightarrow D^* \bar{D}$

As pointed out in Sec. IID, in the limit of zero vector meson masses, degenerate pseudoscalar meson masses, and SU(4) invariant coupling constants, all amplitudes for the three  $J/\psi$  absorption processes shown in Fig. 1 should satisfy the current conservation condition of Eq. (24). Here, we consider the process  $\pi\psi \rightarrow D^* \bar{D}$  as an example and explicitly check the current conservation condition in both our approach and that of Ref. [17]. For simplicity, we take all meson masses to be zero.

#### 1. Our approach

The three amplitudes for the process  $\pi\psi \rightarrow D^* \bar{D}$  are shown in Eq. (15). Multiplying them by  $p_{2\nu}$  and omitting the common factor  $-g_{\pi DD^*} g_{\psi DD}$ , we obtain

$$\begin{aligned} \mathcal{M}_{1a}^{\nu\lambda} p_{2\nu} &= \frac{p_2 \cdot (p_1 - p_3 + p_4)}{t} (-2p_1 + p_3)^\lambda = (2p_1 - p_3)^\lambda, \\ \mathcal{M}_{1b}^{\nu\lambda} p_{2\nu} &= \frac{(p_1 + p_4)^\alpha}{u} g_{\alpha\beta} \left[ (-p_2 - p_3)^\beta g^{\nu\lambda} + (-p_1 + p_2 + p_4)^\lambda g^{\beta\nu} + (p_1 + p_3 - p_4)^\nu g^{\beta\lambda} \right] p_{2\nu} \\ &= \frac{(p_1 + p_4)_\beta}{u} \left[ -p_3^\beta p_2^\lambda + p_2^\beta (-p_1 + p_4)^\lambda - u g^{\beta\lambda} \right] = \left[ \left( \frac{-s+t}{2u} \right) p_3 - p_1 - p_4 \right]^\lambda, \\ \mathcal{M}_{1c}^{\nu\lambda} p_{2\nu} &= p_2^\lambda. \end{aligned} \quad (\text{B8})$$

Their sum is given by

$$\mathcal{M}_1^{\nu\lambda} p_{2\nu} = \left( \frac{-s+t}{2u} \right) p_3^\lambda \Rightarrow 0. \quad (\text{B9})$$

As indicated in the last step, it goes to zero when contracting with the external polarization  $\epsilon_{3\lambda}$  of the charm vector meson. It is also straightforward to verify the current conservation condition for  $M_1^{\nu\lambda} p_{3\lambda}$  as shown later in Eq. (B16).

## 2. Approach of Ref. [17]

Using the interaction Lagrangians of Ref. [17] as explained in the above, we obtain the following corresponding amplitudes for Eqs. (B3), (B4), (B5), and (B7):

$$\begin{aligned} m_{1a}^{\nu\lambda} &= \frac{g'_{\pi DD^*}}{2} g'_{\psi DD} (-2p_1 + p_3)^\lambda \left( \frac{1}{t - m_D^2} \right) (p_1 - p_3 + p_4)^\nu, \\ m_{1b}^{\nu\lambda} &= \frac{g'_{\pi DD^*}}{2} g'_{\psi D^* D} (p_1 + p_4)^\alpha \left( \frac{1}{u - m_{D^*}^2} \right) \left[ g_{\alpha\beta} - \frac{(p_1 - p_4)_\alpha (p_1 - p_4)_\beta}{m_{D^*}^2} \right] \\ &\quad \times \left[ -p_3^\beta g^{\nu\lambda} + (-p_1 + p_4)^\lambda g^{\beta\nu} + (p_1 + p_3 - p_4)^\nu g^{\beta\lambda} \right], \\ m_{1c}^{\nu\lambda} &= -g'_{\pi DD^*} g'_{\psi DD} g^{\nu\lambda}. \end{aligned} \quad (\text{B10})$$

Taking  $g'_{\psi D^* D} = g'_{\psi DD}$  as in Eq. (5) of Ref. [17] and omitting the common factor  $g_{\pi DD^*} g_{\psi DD}/2$ , we obtain

$$\begin{aligned} m_{1a}^{\nu\lambda} p_{2\nu} &= (2p_1 - p_3)^\lambda, \\ m_{1b}^{\nu\lambda} p_{2\nu} &= \frac{(p_1 + p_4)^\alpha}{u} g_{\alpha\beta} \left[ -p_3^\beta g^{\nu\lambda} + (-p_1 + p_4)^\lambda g^{\beta\nu} + (p_1 + p_3 - p_4)^\nu g^{\beta\lambda} \right] p_{2\nu} \\ &= \frac{(p_1 + p_4)_\beta}{u} \left[ -p_3^\beta p_2^\lambda + p_2^\beta (-p_1 + p_4)^\lambda - u g^{\beta\lambda} \right] = \left[ \left( \frac{-s+t}{2u} \right) p_3 - p_1 - p_4 \right]^\lambda, \\ m_{1c}^{\nu\lambda} p_{2\nu} &= -2p_2^\lambda. \end{aligned} \quad (\text{B11})$$

Their sum is thus

$$m_1^{\nu\lambda} p_{2\nu} = \left[ \left( \frac{-s+t}{2u} \right) p_3 - 3p_2 \right]^\lambda \Rightarrow -3p_2^\lambda. \quad (\text{B12})$$

When contracting with the external polarization  $\epsilon_{3\lambda}$  of the charm vector meson, the first term vanishes but the second remains as shown in the last step. Therefore, the current conservation condition is not satisfied in Ref. [17].

To understand the above results, we compare the amplitudes given in Eq. (B11) against Eq. (B8) and note the following two differences. (i) In  $m_{1b}$  of Eq. (B11), the two terms  $-p_3^\beta g^{\nu\lambda} + p_2^\lambda g^{\beta\nu}$  involving the four-momentum of  $\psi$  in the  $\psi D^* D$  vertex are missing. (ii)  $m_{1c}$  in Eq. (B11) is a factor of  $-2$  larger than ours [also see the comment after Eq. (B7)]. In calculating  $m_1^{\nu\lambda} p_{2\nu}$ , the difference in (i) does not matter as it accidentally gives  $(-p_2^\beta p_2^\lambda + p_2^\lambda p_2^\beta) = 0$ . The failure of satisfying the current conservation condition in Ref. [17] is thus due to the difference in (ii).



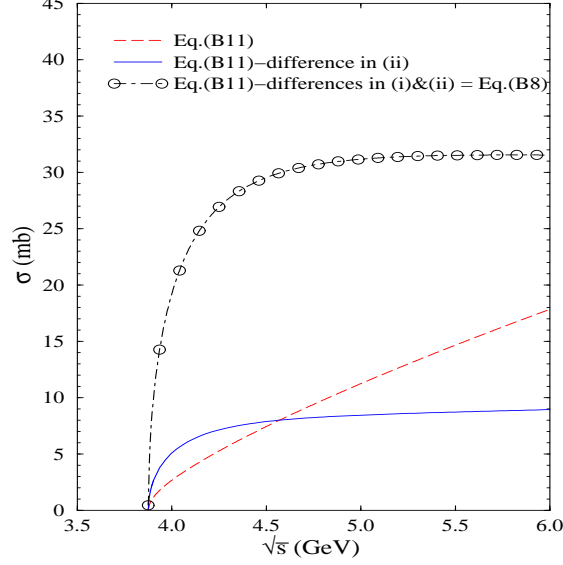


FIG. 6. Comparison of  $J/\psi$  absorption cross section by pions. The dashed curve represents the result of Eq. (B11) based on the Lagrangian from Ref. [17]. The solid curve is the result from Eq. (B11) by dividing the amplitude  $m_{1c}$  by a factor of  $-2$ , which reproduces the result from Ref. [17]. The circled curve is the result from Eq. (B8) based on our Lagrangian.

To see this more clearly, we show in Fig. 6 by the dashed curve the cross section for  $J/\psi$  absorption by pions obtained from the amplitudes given in Eq.(B11) and using the coupling constants  $g'_{\pi DD^*} = 8.8$  and  $g'_{\psi DD} = g'_{\psi D^* D^*} = 7.7$  given in Ref. [17]. However, the results are different from that shown in Fig. 1 of Ref. [17], which is reproduced here by the solid curve in Fig. 6. We have found that to reproduce the results in Ref. [17] requires dividing the amplitude  $m_{1c}$  in Eq. (B11) by  $-2$ .

We note that although the current conservation condition is satisfied for  $m_1^{\nu\lambda} p_{2\nu}$  when  $m_{1c}$  in Eq. (B11) is divided by a factor of  $-2$ , the current conservation condition for  $m_1^{\nu\lambda} p_{3\lambda}$  remains violated. This is shown explicitly in the following.

From the amplitudes shown in Eq. (B11), we have, after omitting the common factor  $g'_{\pi DD^*} g'_{\psi DD}/2$ ,

$$\begin{aligned}
m_{1a}^{\nu\lambda} p_{3\lambda} &= \frac{p_3 \cdot (-2p_1 + p_3)}{t} (p_1 - p_3 + p_4)^\nu = (p_1 - p_3 + p_4)^\nu, \\
m_{1b}^{\nu\lambda} p_{3\lambda} &= \frac{(p_1 + p_4)^\alpha}{u} g_{\alpha\beta} \left[ -p_3^\beta g^{\nu\lambda} + (-p_1 + p_4)^\lambda g^{\beta\nu} + (p_1 + p_3 - p_4)^\nu g^{\beta\lambda} \right] p_{3\lambda} \\
&= \frac{(p_1 + p_4)_\beta}{u} \left[ p_3 \cdot (-p_1 + p_4) g^{\nu\beta} + p_3^\beta (p_1 - p_4)^\nu \right] = \left[ \frac{(p_1 + p_4)}{-2} + \left( \frac{s-t}{2u} \right) (p_1 - p_4) \right]^\nu, \\
m_{1c}^{\nu\lambda} p_{3\lambda} &\rightarrow m_{1c}^{\nu\lambda} p_{3\lambda} / (-2) = p_3^\nu.
\end{aligned} \tag{B13}$$

Their sum is

$$m_1^{\nu\lambda} p_{3\lambda} = \left[ \frac{(p_1 + p_4)}{2} + \left( \frac{s-t}{2u} \right) (p_1 - p_4) \right]^\nu, \tag{B14}$$

which does not go to zero when contracting with the external polarization  $\epsilon_{2\nu}$ .

On the other hand, if we also add the two missing terms in  $l_{\psi D^* D^*}$  according to our Eq. (9), i.e., adding  $-p_2^\beta g^{\nu\lambda} + p_2^\lambda g^{\beta\nu}$  to the  $\psi D^* D^*$  vertex in  $m_{2b}$  in Eq.(B11), we then have the following additional contribution to  $m_{1b}^{\nu\lambda} p_{3\lambda}$ :

$$\frac{(p_1 + p_4)_\beta}{u} (-p_2^\beta p_3^\nu + p_2 \cdot p_3 g^{\beta\nu}) = \left[ \frac{(p_1 + p_4)}{-2} - \left( \frac{s-t}{2u} \right) p_3 \right]^\nu. \quad (\text{B15})$$

Combining the above two results gives

$$m_1^{\nu\lambda} p_{3\lambda} = \left( \frac{s-t}{2u} \right) (p_1 - p_4 - p_3)^\nu = \left( \frac{s-t}{2u} \right) (-p_2^\nu) \Rightarrow 0. \quad (\text{B16})$$

As shown in the last step, it vanishes when contracting with the external polarization  $\epsilon_{2\nu}$ . The results after eliminating both differences (i) and (ii), i.e., using our amplitudes given in Eq. (B8), are shown by the circled curve in Fig. 6, which is only slightly different from our results shown in Fig. 2 due to the different value for  $g_{\psi DD}$  (7.7 vs 7.64).

## REFERENCES

- [1] T. Matsui and H. Satz, Phys. Lett. B **178**, 416 (1986).
- [2] NA38 Collaboration, M. C. Abreu *et al.*, Z. Phys. C **38**, 117 (1988); C. Baglin *et al.*, Phys. Lett. B **220**, 471 (1989).
- [3] C. Baglin *et al.*, Phys. Lett. B **270**, 105 (1991); **345**, 617 (1995).
- [4] NA50 Collaboration, M. Gonin *et al.*, Nucl. Phys. **A610**, 404c (1996); NA50 Collaboration, M. C. Abreu *et al.*, Phys. Lett. B **450**, 456 (1999).
- [5] D. Kharzeev, C. Lourenço, M. Nardi, and H. Satz, Z. Phys. C **74**, 307 (1997).
- [6] See, e.g., R. Vogt, Phys. Rep. **310**, 197 (1999).
- [7] J.-P. Blaizot and J.-Y. Ollitrault, Phys. Rev. Lett. **77**, 1703 (1996).
- [8] C.-Y. Wong, Nucl. Phys. **A630**, 487 (1998).
- [9] W. Cassing and C. M. Ko, Phys. Lett. B **396**, 39 (1997); W. Cassing and E. L. Bratkovskaya, Nucl. Phys. **A623**, 570 (1997).
- [10] N. Armesto and A. Capella, Phys. Lett. B **430**, 23 (1998).
- [11] C. M. Ko, X.-N. Wang, B. Zhang, and X. F. Zhang, Phys. Lett. B **444**, 237 (1998).
- [12] P. Braun-Munzinger and K. Redlich, Nucl. Phys. **A661**, 546 (1999).
- [13] K. Martins, D. Blaschke, and E. Quack, Phys. Rev. C **51**, 2723 (1995).
- [14] C.-Y. Wong, E. S. Swanson, and T. Barnes, hep-ph/9912431.
- [15] D. Kharzeev and H. Satz, Phys. Lett. B **334**, 155 (1994).
- [16] S. G. Matinyan and B. Müller, Phys. Rev. C **58**, 2994 (1998). Note that some coupling constants have a factor of 2 difference in the definitions.
- [17] K. Haglin, Phys. Rev. C **61**, 031902 (2000).
- [18] Z. Lin, C. M. Ko, and B. Zhang, Phys. Rev. C **61**, 024904 (2000).
- [19] P. Colangelo, F. De Fazio, and G. Nardulli, Phys. Lett. B **334**, 175 (1994); V. M. Belyaev, V. M. Braun, A. Khodjamirian, and R. Ruckl, Phys. Rev. D **51**, 6177 (1995).
- [20] J. Vermaseren, computer code FORM, 1989. The free version of the software is available on the internet at <ftp://hep.itp.tuwien.ac.at/pub/Form/PC/>.
- [21] D. E. Kahana and S. H. Kahana, Phys. Rev. C **59**, 1651 (1999); B.-H. Sa, A. Tai, H. Wang, and F.-H. Liu, *ibid.* **59**, 2728 (1999); C. Spieles, R. Vogt, L. Gerland, S. A. Bass, M. Bleicher, H. Stöcker, and W. Greiner, *ibid.* **60**, 054901 (1999).
- [22] C. Song and V. Koch, Phys. Rev. C **55**, 3026 (1997).
- [23] J. Kapusta, P. Lichard, and D. Seibert, Phys. Rev. D **44**, 2774 (1991); **47**, 4171(E) (1993).
- [24] G. E. Brown and M. Rho, Phys. Rev. Lett. **66**, 2720 (1991); T. Hatsuda and S. H. Lee, Phys. Rev. C **46**, R34 (1992); M. Asakawa, C. M. Ko, P. Lévai, and X. J. Qiu, *ibid.* **46**, R1159 (1992); C. M. Ko, V. Koch, and G. Q. Li, Ann. Rev. Nucl. Part. Sci. **47**, 505 (1997).
- [25] CERES Collaboration, G. Agakishiev *et al.*, Phys. Rev. Lett. **75**, 1272 (1995); CERES Collaboration, P. Wurm *et al.*, Nucl. Phys. **A590**, 103c (1995).
- [26] L.-H. Chan, Phys. Rev. D **55**, 5362 (1997).
- [27] F. Klingl, N. Kaiser, and W. Weise, Z. Phys. A **356**, 193 (1996).
- [28] K. Haglin and C. Gale, nucl-th/0002029.